ISSN 1990-7931, Russian Journal of Physical Chemistry B, 2024, Vol. 18, No. 6, pp. 1486–1495. © Pleiades Publishing, Ltd., 2024.

STRUCTURE OF CHEMICAL COMPOUNDS, QUANTUM CHEMISTRY, SPECTROSCOPY

A Generalized Method for the Estimation of the Intensity of Electron-Phonon Interaction in Photosynthetic Pigments using the Evolutionary Optimization Algorithm

V. A. Kurkov[a, b], D. D. Chesalin[a], A. P. Razjivin[c], U. A. Shkirina[a, d], and R. Y. Pishchalnikov[a, *]

[a] *Prokhorov General Physics Institute of the Russian Academy of Sciences, Moscow, 119991 Russia*

[b] *Moscow Institute of Physics and Technology (National Research University), Dolgoprudny, 141701 Russia*

[c] *Belozersky Research Institute of Physico-Chemical Biology, Lomonosov Moscow State University, Moscow, 119992 Russia*

[d] *Department of Mechanics and Mathematics, Lomonosov Moscow State University, Moscow, 119991 Russia*

**e-mail: rpishchal@kapella.gpi.ru*

Received December 15, 2023; revised April 3, 2024; accepted April 22, 2024

Abstract—Modeling the optical response of photosynthetic pigments is an integral part of the study of fundamental physical processes of interaction between multi-atomic molecules and the external electromagnetic field. In contrast to ab initio methods for calculating the ground and excited states of a molecule, the use of semiclassical quantum theories allows us to use characteristic functions, such as spectral density, to calculate absorption spectra rather than considering the full set of electron and atom configurations. The main disadvantage of this approach is the comparison of calculated and experimental spectra and, as a consequence, the need to justify the uniqueness of the obtained parameters of the system under study and to evaluate their statistical significance. In order to improve the quality of the optical response calculation, a heuristic evolutionary optimization algorithm was used in this work, which minimizes the difference between the measured and theoretical spectra by determining the most appropriate set of model parameters. It is shown that, using as an example the spectra of photosynthetic pigments measured in different solvents, the optimization of modeling allowed us to obtain a good agreement between the calculated and experimental data and to unambiguously determine the electron-phonon interaction coefficients for the electronic excited states of chlorophyll, lutein and β-carotene.

Keywords: chlorophyll *a*, lutein, β-carotene, spectral density, multimode Brownian oscillator model, optimization algorithms, differential evolution

DOI: 10.1134/S1990793124701422

INTRODUCTION

The analysis and interpretation of spectroscopy data of both monomeric pigments in solvents and pigment-protein complexes (PPCs) plays a key role in studies of the primary processes of photosynthesis [1–3]. PPCs of plants, bacteria and blue-green algae exhibit a wide variety of optical properties and packaging of pigments in the protein matrix [4, 5]. Chlorophylls (Chl), bacteriochlorophylls and carotenoids are the main pigments providing optical activity of PPC in the visible spectral range [6]. The specific features of the chemical structure of photosynthetic pigments allow them to efficiently absorb external electromagnetic radiation, converting it into the energy of electronic excitations [7]. The interaction of pigments inside PPC leads to the formation of quasi-particles – excitons, possessing different degrees of delocalization in the complexes, which results in a change in the optical properties of PBC compared to monomeric pigments [8–10]. Eventually, the diversity of light-harvesting complexes and their mutual arrangement in the membranes of photosynthetic organisms ensure efficient transfer of absorbed energy to specialized protein structures—reaction centers, where chemical processes of charge separation take place [11, 12].

Theoretical analysis of optical properties of PPCs is impossible without knowledge of basic quantum characteristics of pigments, such as the energy of electronic excited states and their lifetime, as well as the magnitude and direction of dipole moment transitions from one state to another [13]. These parameters determine the profile of the pigment absorption spectra and its potential ability to exchange energy with other pigments in the PPC. The application of modern ab initio quantum calculations [14–16] for modeling the electronic and vibrational excited states of organic pigments allows us to evaluate the optical properties of monomeric molecules with high accuracy; however, such calculations for systems of interacting pigments become very energy- and time-consuming.

To speed up calculations, an alternative to ab initio simulations can be considered modeling the optical

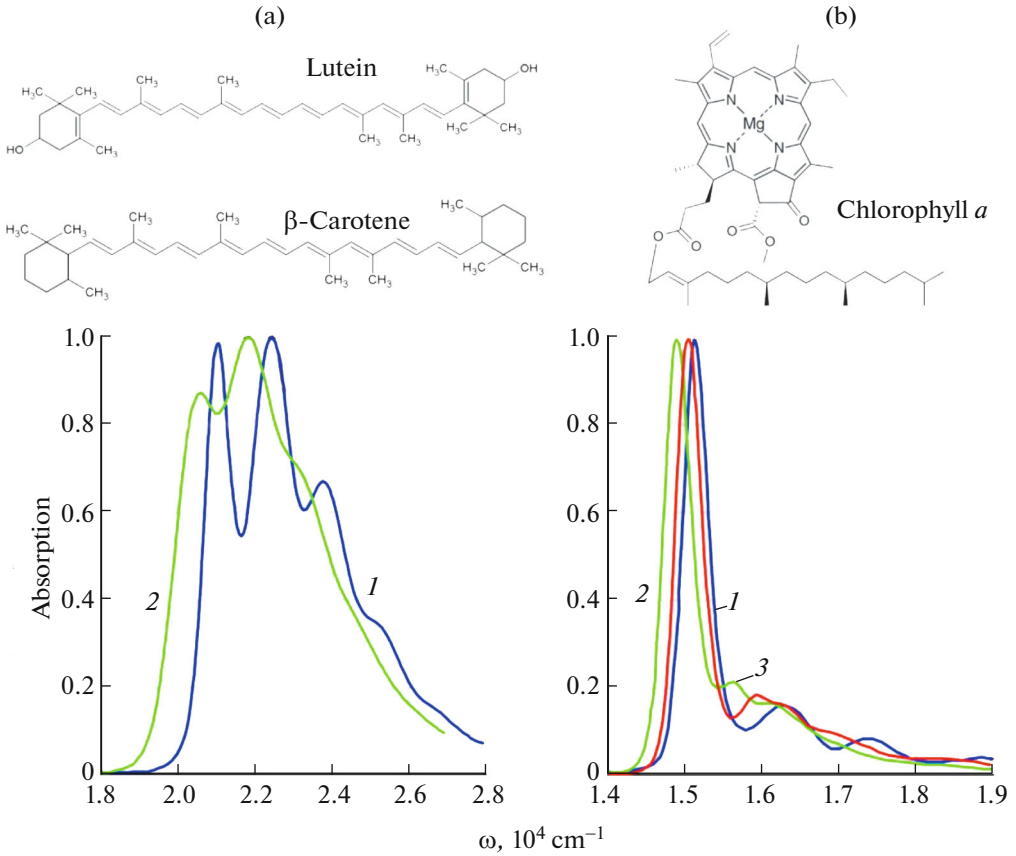

Fig. 1. Chemical structure and absorption spectra of the photosynthetic pigments measured at room temperature: lutein (*1*) and β-carotene (*2*) in THF (a) and Chl*a* in (*1*) diethyl ether, (*2*) pyridine and (*3*) THF (b).

response using the semiclassical quantum theory of the interaction of electromagnetic radiation with matter [17]. This theory is based on the concept of the spectral density function, which carries information about the effective vibrational modes that characterize the electronic excitation of the molecule under study. Each vibrational mode is defined by three quantities: frequency, damping coefficient and intensity of interaction with electronic excitation (Huang–Rhys factor) [18]. Due to the phenomenological nature of this approach, a comparison of measured and calculated spectra is necessary to estimate the parameters of the system under study. The process of fitting the spectra is associated with the search of virtually infinite number of possible parameter values and comparison of the obtained modeling results with experimental data for each set of potential "ideal" parameters of the system.

As the results of the research show, the problem of modeling the optical properties of photosynthetic pigments can be solved using evolutionary algorithms, the heuristic nature of which makes it possible to tune the optimal mode of the optimizer without going into the nuances and details of a particular problem. Differential evolution (DE) is one of the most widely used optimization methods [19, 20]. The algorithm is based on a set of specific methods of selecting a mutant vector of optimized parameters [21].

Using the example of modeling the absorption spectra of lutein, β-carotene and Chl*a* taken at room temperature in different solvents (Fig. 1), we demonstrate that the simultaneous application of semiclassical quantum theory and differential evolution method allows us to determine statistically significant spectral density parameters for each pigment-solvent combination [22]. Moreover, the application of the optimization algorithm, in contrast to the conventional calculation of spectra, allows us to set the initial spectral density with an equidistant set of vibrational frequencies with fixed values of the Huang–Rhys factors, which either becomes significant or negligibly small in the process of fitting the experimental spectra. As a result, the obtained spectral density can be regarded as a characteristic function describing the degree of electron-phonon interaction for each vibronic mode with an electronic transition.

MATERIALS AND METHODS

Differential Evolution Algorithm

For modeling the absorption spectra of pigments, the classical version of the DE designed to find the

global minimum of functions of many variables was taken as a basis. Its advantage is that the minimized function can be nonlinear, nondifferentiable and multimodal. With a correctly specified physical model, a large number of free parameters can only increase the running time of the algorithm, while leaving its final accuracy acceptable. To start the optimization of simulations, the target function, free parameters and their search range must be set before running the program [18, 23]. If $\sigma^{exp}(\omega_m)$ is the experimental spectrum, $\sigma^{exp}(\omega_m, x_i)$ is the simulated spectrum, x_i is the set of quantum model parameters to be optimized, and ω_m is the frequency range of the measured spectrum, then the target minimized function will be:

$$\chi^2(x_i) = \frac{1}{M}\sum_{m=1}^{M}\left(\sigma^{exp}(\omega_m) - \sigma(\omega_m, x_i)\right)^2. \quad (1)$$

At the initial stage of DE, a set of vectors is created in the n-dimensional space, where n is the number of free parameters, for each of which the value of the target function is calculated. The best one (i.e. the one with the smallest function value) is taken into the next generation, then a new generation of vectors is created by mutation and crossing, the values of which will be compared with the best vector from the previous one, after which the best vector at the moment will be selected again. The cycle of sequential procedures of mutation, crossover and selection will operate until the calculations stop. The end of the program can be initially set by the number of generations or by reaching a sufficient value of the target function.

The Multimode Brownian Oscillators Theory

The semiclassical theory of multimode Brownian oscillators was used to calculate the profile of the absorption spectra. This theory usually considers a system of two electronic levels (ground and excited), each of which interacts with a set of vibrational states of the molecular backbone and the nearest protein environment or solvent, which in turn is also modeled by a set of damped oscillators [17]. The external influence of the electric field is considered as a perturbation for the system of electronic levels, which is not quantized and represented as a Gaussian packet $E(\mathbf{r},t)$. If the polarization of the medium is decomposed by degrees of perturbation as

$$P(\mathbf{r},t) = P(\mathbf{r},t)^{(1)} + P(\mathbf{r},t)^{(2)} + P(\mathbf{r},t)^{(3)} + \cdots, \quad (2)$$

then the expression corresponding to the first-order polarization is written in the form

$$P(\mathbf{r},t)^{(1)} = -\frac{i}{\hbar}\int_0^\infty dt_1 E(\mathbf{r}, t-t_1)S^{(1)}(t_1), \quad (3)$$

where $S^{(1)}(t_1)$ is the optical response function of the system of electronic levels. Knowing the optical response function, we can calculate the absorption spectrum $\sigma(\omega)$, corresponding to the transition of the system from the ground state to the excited state by the formula

$$\sigma(\omega) = \int_{-\infty}^{\infty} dt S^{(1)}(t_1)e^{i\omega t}. \quad (4)$$

The methods to calculate $S^{(1)}(t_1)$ are described in many publications [1, 2, 17]. In general, formula (4), which is suitable for numerical modeling, is expressed through the correlation function $g(t)$ of the dipole moment of the transition from the ground to the excited state:

$$g(t) = \frac{1}{2\pi}\int_{-\infty}^{\infty} d\omega \frac{1-\cos\omega t}{\omega^2}\coth(\beta\hbar\omega/2)C''(\omega) - \frac{i}{2\pi}\int_{-\infty}^{\infty} d\omega \frac{\sin(\omega t)-\omega t}{\omega^2}C''(\omega), \quad (5)$$

this function depends on the temperature ($1/\beta = kT$) d on the spectral density of the electron transition.

The expression for the spectral density can be obtained by the method of continuum integration [15] and is given as follows:

$$C''(\omega) = \sum_j \frac{2S_j\omega_j^3\omega\gamma_j}{\left(\omega_j^2-\omega^2\right)^2 + \omega^2\gamma_j^2}, \quad (6)$$

where $\{\omega_j, S_j, \gamma_j\}$ is the set of parameters characterizing vibrational modes of the pigment; ω_j is the frequency of the jth mode, S_j is the Huang–Rhys factor of the jth mode, γ_j is the damping coefficient for the jth mode. To obtain the most realistic profile of the absorption spectra, it is also necessary to take into account the effect of inhomogeneous broadening, which is modeled by adding an exponential factor $e^{-(\Delta t)^2/2}$ to the expression for the $\sigma(\omega)$, where $\Delta = \mathrm{FWHM}/2\sqrt{2\ln 2}$ and FWHM defines the full width at half maximum of the Gaussian distribution for the values of Ω_{eg}. Thus, the expression for calculating the absorption spectra takes from [24]:

$$\sigma(\omega) = \frac{1}{\pi}\mathrm{Re}\int_0^\infty dt \exp\{i(\omega-\Omega_{eg})t\}\exp\{-g(t)\}\exp\left\{-\frac{1}{2}(\Delta t)^2\right\}. \quad (7)$$

RESULTS

In the visible region, the absorption spectra of carotenoids are associated with the $S_0 \rightarrow S_2$ electronic transition, while the $S_0 \rightarrow S_1$ transition is forbidden by symmetry rules [25]. Chl*a* is optically active in both the high-frequency (Soret band) and low-frequency regions of the visible range. In this work, only the

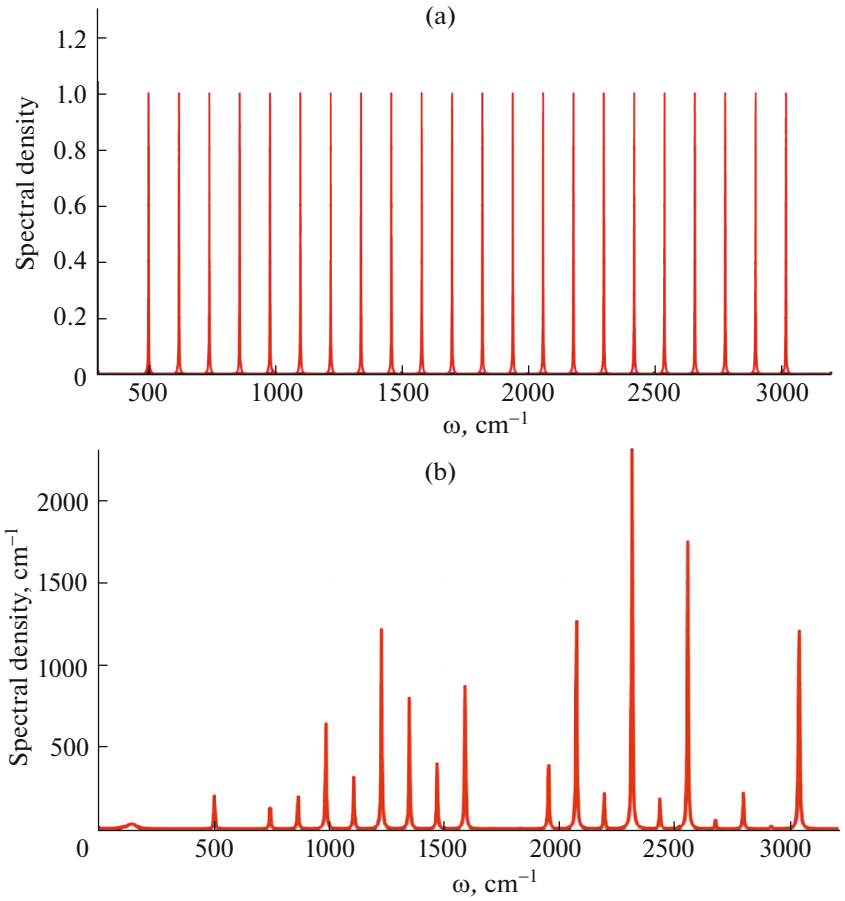

Fig. 2. The generalized spectral density functions before the start of spectrum modeling (a) and after modeling (b). Initially, vibronic frequencies are uniformly distributed in the range from 500 to 3020 cm^{-1}, the damping coefficient is the same for each mode and is fixed, the Huang–Rhys factors are free parameters (this fact is reflected by the same intensities for each mode). After the end of optimization, the values of the Huang–Rhys factors are determined and correspond to the theoretical spectrum, which maximally coincides with the experimental one.

$S_0 \rightarrow Q_y$ bands of the low-frequency electronic transition of Chl*a* were taken into account. The absorption spectra of lutein and β-carotene in tetrahydrofuran (THF) and Chl*a* in diethyl ether, pyridine, and THF measured at room temperature were used for the simulations. The initial values of the frequencies of vibrational modes in the spectral density (Fig. 2) were set in the range of 500 to 3020 cm^{-1} with a uniform step of 120 cm^{-1}. Thus, the overall number of free parameters is $D = 27$, specifically, 22 electron-phonon interaction intensities for each mode (Huang–Rhys factors), the electron transition energy between the ground and excited states, Ω_{eg}, $FWHM_{\Omega}$ of the inhomogeneous broadening, and three values for the low-energy vibronic mode: $\{\omega_{low}, S_{low}, \gamma_{low}\}$. The settings of the algorithm parameters are similar to those used in computing the linear optical response [18, 23] for a system in which the spectral density was calculated with a fixed set of relevant vibrational modes. DE/best/1/bin was used to perform the simulations with the weighting factor $F = 0.55$ and crossover probability $Cr = 0.9$. The overall number of generations is fixed for each run of the program $P = 300$. The number of calls of the computational function for one run of the optimization program is determined through the number of free parameters D and is equal to $K = 10PD$. The results of spectra modeling for all "pigment–solvent" combinations are shown in Figs. 3 and 4. The parameters of the quantum models for each spectrum are presented in Table 1. These values correspond to the lowest value of the function $\chi^2(x_i)$ obtained after 10 runs of DE algorithm.

As can be seen from the presented results, for Chl*a* and carotenoids were of the same order, indicating the universality of the method used for the different type of pigments. Taking into account that the simulated spectra are within different energy ranges (carotenoids from 19000 to 26000 cm^{-1}, Chl*a* from 14000 to 17000 cm^{-1}), it can be stated that the optimization algorithm converges steadily for electronic transitions Ω_{eg} with val-

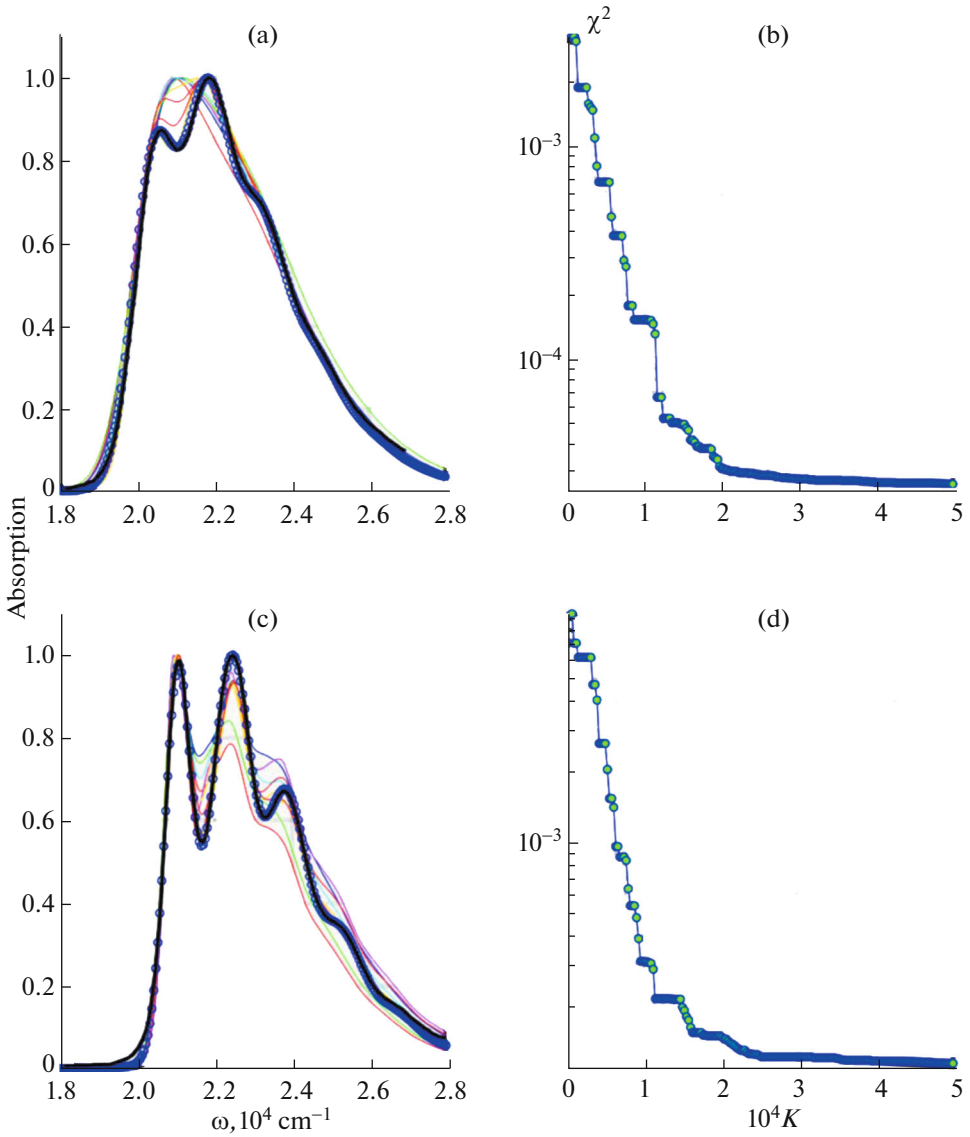

Fig. 3. Result of the modeling of lutein (a) and β-carotene (c) absorption spectra in THF. Thin lines indicate intermediate results of calculations for the first seven generations of DE. The dependence of the minimized discrepancy function between the experimental and theoretical spectra on the number of calls of the spectra simulation procedure for lutein and β-carotene is shown in graphs (b) and (d).

ues in the visible range. A similar conclusion about the versatility of the method can be made for modeling different types of solvents: diethyl ether and THF are nonpolar, while pyridine is polar. In all plots of Figs. 3 and 4, the discrepancy function after 300 generations asymptotically approaches the limit, which is determined by the noise of the measured spectra.

The initial spectral density for each optimization run was the same (Fig. 2a). The final result of the optimization is 27 parameters of the quantum model, averaged after 10 program runs, on the basis of which the resulting spectral density is calculated (Fig. 2b). The calculated spectral densities for lutein and β-carotene, as well as for Chl*a* in diethyl ether, pyridine, and THF after each DE run are shown in Figs. 5 and 6. The final results of the optimization are independent of the initial conditions. The arrows indicate the frequency regions where maximum differences are observed for pigments in different solvents.

DISCUSSION

Linear optical response modeling using differential evolution has already been successfully applied by our research team to analyze the absorption spectra of astaxanthin [18] in polar and nonpolar solvents, a keto-carotenoid produced by algae and yeast fungus.

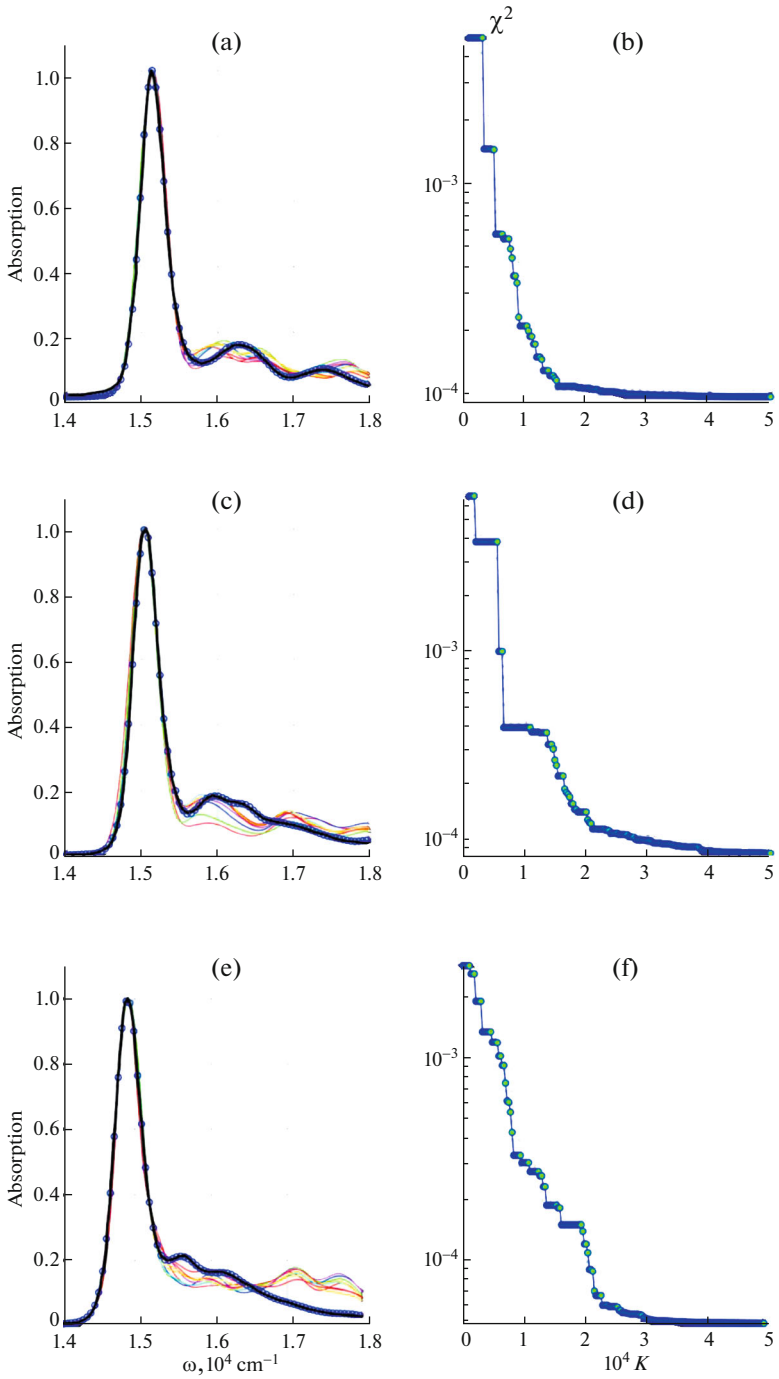

Fig. 4. Result of the modeling of Chl *a* absorption spectra in diethyl ether (a), pyridine (c) and in THF (e). Thin lines indicate intermediate results of calculations for the first seven generations of DE. The dependence of the minimized discrepancy function between the experimental and theoretical spectra on the number of calls of the spectra simulation procedure for Chl *a* spectra in each solvent is shown in graphs (b), (d) and (f), respectively.

In this work, the spectral density was used for which the number of vibronic modes was fixed and equal to eight. It is known that carotenoid-type molecules are characterized by four main frequencies: vibrations of double and single carbon bonds, as well as methyl groups and hydrogen. Taking into account two overtones and another frequency corresponding to the sum of double and single carbon bonds, a good agreement between theory and experiment was obtained. However, in this study we use a more general approach for the spectral density, not limiting ourselves to a finite set of modes at certain frequencies, but setting a comb

Table 1. Parameters of the semiclassical theory optimized by differential evolution on the basis of which the absorption spectra of β-carotene and lutein in THF and Chl*a* in pyridine, diethyl ether and THF are calculated

Free parameters		β-carotene–THF	Lutein–THF	Chl*a*–THF	Chl*a*–pyridine	Chl*a*–diethyl ether
1	Ω_{eg}	22463.75	23175.85	15836.04	15518.32	15763.26
2	$FWHM_{\Omega}$	1307.67	793.40	50.15	357.86	279.14
3	ω_{low}	175.87	82.94	163.13	295.85	252.96
4	S_{low}	0.025	0.24	0.49	0.16	0.22
5	γ_{low}	63.42	287.75	182.48	37.20	211.24
6	S_{500}	0.00057	0.00012	0.059	0.0061	0.051
7	S_{620}	0.00031	0.00088	0.00029	0.053	0.0014
8	S_{740}	0.00050	0.0018	0.023	0.12	0.025
9	S_{860}	0.00022	0.21	0.050	0.018	0.11
10	S_{980}	0.00072	0.027	0.032	0.022	0.035
11	S_{1100}	0.048	0.21	0.054	0.052	0.014
12	S_{1220}	0.30	0.27	0.050	0.028	0.057
13	S_{1340}	0.52	0.0060	0.037	0.057	0.054
14	S_{1460}	0.045	0.0042	0.031	0.00073	0.0092
15	S_{1580}	0.13	0.49	0.018	0.047	0.012
16	S_{1700}	0.014	0.13	0.0044	0.010	0.053
17	S_{1820}	0.00078	1.18e–005	0.0070	0.0095	0.00019
18	S_{1940}	0.14	0.015	0.0078	0.015	0.0030
19	S_{2060}	0.032	0.0024	0.016	0.011	0.043
20	S_{2180}	0.0017	1.07e–006	0.033	0.0017	0.0017
21	S_{2300}	0.0017	0.0023	0.0039	0.012	0.0040
22	S_{2420}	3.50e–005	0.029	0.032	0.00096	0.00065
23	S_{2540}	3.23e–005	0.0059	0.0043	0.00054	0.023
24	S_{2660}	1.33e–005	0.0033	0.0084	0.0057	6.77e–006
25	S_{2780}	7.38e–006	3.29e–005	0.00097	0.00013	0.00098
26	S_{2900}	0.021	6.76e–005	5.71e–005	8.47e–006	0.0041
27	S_{3020}	0.051	0.076	0.016	0.012	0.017

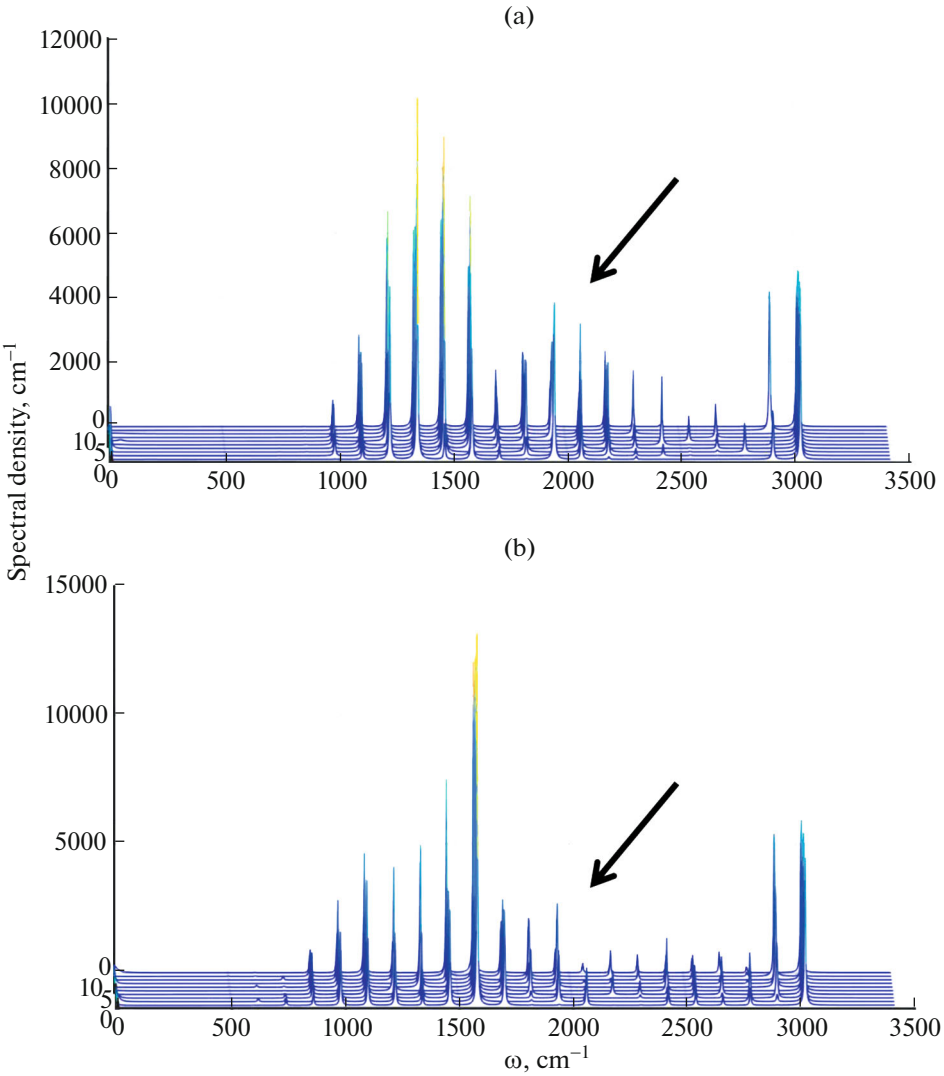

Fig. 5. Spectral densities for lutein (a) and β-carotene (b) in THF obtained after 10 runs of the optimization algorithm. In all cases, the magnitude of the discrepancy did not exceed 10^{-4}. The arrows indicate the frequency range in which the largest differences are observed.

of vibronic modes with a fixed step in a wide range (Fig. 2a). On the one hand, such calculations become much more time-consuming due to the larger number of free parameters; on the other hand, if the algorithm is properly implemented, the overall accuracy can increase. For example, in a previously published study [26] there is a large discrepancy in the high-energy region because only two vibronic modes of carotenoids without overtones were considered.

It is worth noting that the concept of generalized spectral density can be implemented only with the help of an efficient and robust optimization algorithm, since it is impossible to solve this type of problem analytically or 'manually'. If such modeling of carotenoid spectra measured in different solvents is carried out and a database including spectra, chemical formulas and semiclassical quantum theory parameters in the form of generalized spectral density is created, it will be possible to identify specific regularities and classify the type of immediate environment depending on its influence on the studied pigments on the basis of the obtained and systematized data. It should be emphasized that the accuracy of the results strongly depends on the step between the peaks in the comb (in this work it was constant and equal to 120 cm^{-1}). This value needs to be finely optimized, because if the step is too large, many peaks may be missed, and if it is too small, they may be indistinguishable from each other. Based on the available combed peaks, the final absorption spectrum can be calculated. Obviously, the

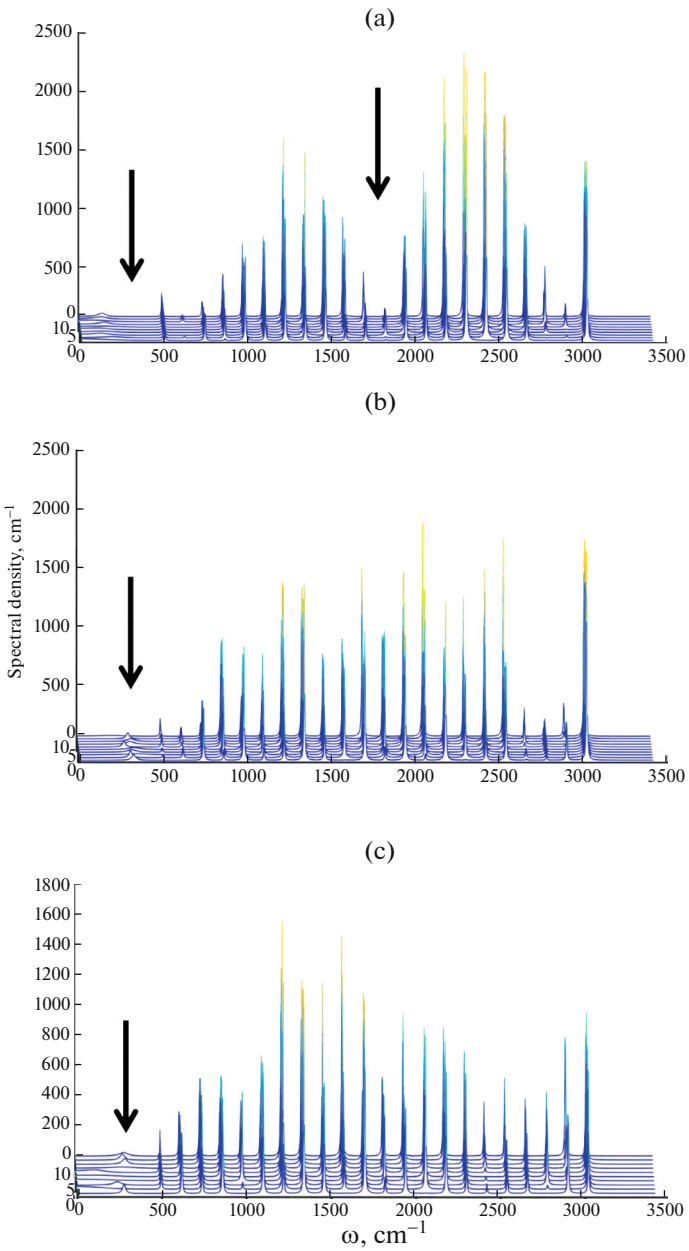

Fig. 6. Spectral densities for Chl *a* in diethyl ether (a), pyridine (b) and THF (c) obtained after 10 runs of the optimization algorithm. In all cases, the magnitude of the discrepancy did not exceed 10^{-4}. The arrows indicate the frequency range in which the largest differences are observed.

idea of the generalized spectral density needs further detailed analysis and elaboration.

Despite the same initial spectral density conditions for all molecule and solvent combinations, different results were obtained at the output of the program, by which each "pigment–solvent" combination can be unambiguously classified. This is confirmed by the small scatter in the data obtained for each pair, as well as the low value of the non-convexity, showing a good agreement between the experimental and calculated data.

CONCLUSIONS

On the example of Chl*a* in three solvents (diethyl ether, pyridine, and THF), as well as lutein and β-carotene in THF, we have shown that the use of a spectral density function of a special kind (in the form of a comb with an equidistant distribution of vibronic

modes in the range from 500 to 3020 cm^{-1}) as an initial condition for multiparametric optimization allowed us to model the experimental data with great accuracy and, at the same time, to obtain statistically distinguishable values of the obtained spectral density. For all pigment–solvent combinations, the electron–phonon interaction intensities defined by Huang–Rhys factors were unambiguously determined.

FUNDING

This work was supported by the Russian Science Foundation (grant no. 22-21-00905, https://rscf.ru/en/project/22-21-00905/).

ETHICS APPROVAL AND CONSENT TO PARTICIPATE

This work does not contain any studies involving human and animal subjects.

CONFLICT OF INTEREST

The authors of this work declare that they have no conflicts of interest.

REFERENCES

1. S. J. Jang and B. Mennucci, Rev. Mod. Phys. **90**, 035003 (2018). https://doi.org/10.1103/RevModPhys.90.035003
2. T. Mirkovic, E. E. Ostroumov, J. M. Anna, et al., Chem. Rev. **117**, 249 (2017). https://doi.org/10.1021/acs.chemrev.6b00002
3. V. V. Gorokhov, P. P. Knox, B. N. Korvatovsky, et al., Russ. J. Phys. Chem. B **17**, 571 (2023). https://doi.org/10.1134/S199079312303020X
4. R. E. Blankenship, *Molecular Mechanisms of Photosynthesis*, 2nd ed. (Wiley-Blackwell, Oxford, 2014).
5. T. Renger, M. E. A. Madjet, M. S. A. Busch, et al., Photosynth. Res. **116**, 367 (2013). https://doi.org/10.1007/s11120-013-9893-3
6. D. A. Cherepanov, G. E. Milanovsky, A. V. Aybush, et al., Russ. J. Phys. Chem. B **17**, 584 (2023). https://doi.org/10.1134/S1990793123030181
7. T. Renger, J. Phys. Chem. B **125**, 6406 (2021). https://doi.org/10.1021/acs.jpcb.1c01479
8. V. I. Novoderezhkin, E. Romero, J. P. Dekker, et al., ChemPhysChem **12**, 681 (2011). https://doi.org/10.1002/cphc.201000830
9. B. Bruggemann, K. Sznee, V. Novoderezhkin, et al., J. Phys. Chem. B **108**, 13536 (2004). https://doi.org/10.1021/jp0401473
10. T. Brixner, R. Hildner, J. Kohler, et al., Adv. Energy Mater. **7**, 1700236 (2017). https://doi.org/10.1002/aenm.201700236
11. R. Croce and H. van Amerongen, Nat. Chem. Biol. **10**, 492 (2014). https://doi.org/10.1038/nchembio.1555
12. D. A. Cherepanov, G. E. Milanovsky, V. A. Nadtochenko, et al., Russ. J. Phys. Chem. B **17**, 594 (2023). https://doi.org/10.1134/S1990793123030193
13. T. R. Nelson, A. J. White, J. A. Bjorgaard, et al., Chem. Rev. **120**, 2215 (2020). https://doi.org/10.1021/acs.chemrev.9b00447
14. D. Cremer and J. A. Pople, J. Am. Chem. Soc. **97**, 1354 (1975). https://doi.org/10.1021/ja00839a011
15. R. Ditchfield, W. J. Hehre, and J. A. Pople, J. Chem. Phys. **54**, 724 (1971). https://doi.org/10.1063/1.1674902
16. M. G. Khrenova, I. V. Polyakov, and A. V. Nemukhin, Russ. J. Phys. Chem. B **16**, 455 (2022). https://doi.org/10.1134/S1990793122030174
17. S. Mukamel, *Principles of Nonlinear Optical Spectroscopy* (Oxford Univ. Press, New York, 1995).
18. D. D. Chesalin, E. A. Kulikov, I. A. Yaroshevich, et al., Swarm Evol. Comput. **75**, 101210 (2022). https://doi.org/10.1016/j.swevo.2022.101210
19. R. Storn, IEEE Trans. Evol. Comput. **3**, 22 (1999). https://doi.org/10.1109/4235.752918
20. R. Storn and K. Price, J. Glob. Opt. **11**, 341 (1997). https://doi.org/10.1023/A:1008202821328
21. K. R. Opara and J. Arabas, Swarm Evol. Comput. **44**, 546 (2019). https://doi.org/10.1016/j.swevo.2018.06.010
22. S. V. Gudkov, R. M. Sarimov, M. E. Astashev, et al., Phys. Usp. **67**, 194 (2024). https://doi.org/10.3367/UFNe.2023.09.039577
23. R. Y. Pishchalnikov, I. A. Yaroshevich, D. V. Zlenko, et al., Photosynth. Res. **156**, 3 (2023). https://doi.org/10.1007/s11120-022-00955-2
24. R. Y. Pishchalnikov, I. A. Yaroshevich, T. A. Slastnikova, et al., Phys. Chem. Chem. Phys. **21**, 25707 (2019). https://doi.org/10.1039/c9cp04508b
25. V. Balevičius, D. Abramavicius, and T. Polívka, J. Phys. Chem. Lett. **7**, 3347 (2016). https://doi.org/10.1021/acs.jpclett.6b01455
26. C. Uragami, K. Saito, M. Yoshizawa, P. Molnar, et al., Arch. Biochem. Biophys. **650**, 49 (2018). https://doi.org/10.1016/j.abb.2018.04.021